Chinese Journal of
POLYMER SCIENCE

ARTICLE

https://doi.org/10.1007/s10118-018-2026-x
Chinese J. Polym. Sci. 2018, 36, 497–504

Phthalonitrile-PPO Blends: Cure Behavior and Properties

Jing-Zhi Ma, Kang Cheng, Jiang-Bo Lv, Chang Chen, Jiang-Huai Hu, Ke Zeng*, and Gang Yang*

State Key Laboratory of Polymer Materials Engineering, College of Polymer Science and Engineering, Sichuan University, Chengdu 610065, China

Abstract Hydroxy-containing low molecular weight poly(2,6-dimethyl-1,4-phenylene oxide) (rPPO) and self-promoted hydroxy-containing phthalonitrile (HPPH) were prepared by redistribution reaction and the simple nucleophilic displacement of a nitro-substituent from 4-nitrophthalonitrile in a dipolar aprotic solvent respectively. The hydroxy-containing phthalonitriles modified by rPPO were prepared by mechanical blending without compatibilizer, followed by heating. The curing behavior was studied using dynamic rheological analysis, and the results showed that the rPPO-modified phthalonitrile exhibited a large processing window (over −67 °C) and complex viscosity (0.18−0.8 Pa·s) at moderate temperatures. After curing at 300 °C, the resulting polymers showed good thermal stability and high modulus as observed by thermogravimetric analysis (TGA) and dynamic mechanical analysis (DMA). The dielectric properties and the morphology of rPPO-modified phthalonitrile networks were studied by dielectric analysis and field-emission scanning electron microscopy (SEM).

Keywords Low molecular weight PPO; Phthalonitrile; Curing behavior; Dielectric properties

Citation: Ma, J. Z.; Cheng, K.; Lv, J. B.; Chen, C.; Hu, J. H.; Zeng, K.; Yang, G. Phthalonitrile-PPO Blends: Cure Behavior and Properties. Chinese J. Polym. Sci. 2018, 36(4), 497–504.

INTRODUCTION

Poly(2,6-dimethyl-1,4-phenylene oxide) (PPO) is one of the high performance thermoplastic resins with outstanding properties, including excellent electrical properties, a low dielectric constant and a low dielectric dissipation factor, as well as excellent mechanical properties, high dimensional stability, low flammability and low moisture uptake[1–3]. Hence, it is a potential candidate as a material for high frequency substrates. However, the high-molecular-weight thermoplastic PPO resin has a number of defects, such as high melt viscosity, poor solvent resistance and relatively poor thermal properties, which determine that it is difficult to directly use PPO for printed circuit boards (PCB)[4, 5].

Thermosetting polymers containing terminal phthalonitrile units are a type of high performance polymers possessing excellent properties, such as high thermal and thermal oxidative stability, excellent mechanical properties, low flammability and low melt viscosity[6–11]. These properties endow phthalonitrile (PN) with many potential uses, including composite matrices, adhesives, structural applications, aerospace and marine[12–16]. But, the polymerization of the neat PN resins is extremely tardy and demands several days at elevated temperatures before a vitrified product is obtained, which seriously restricts the resin applications[17]. During the past years, researchers had developed many different types of curing additives, such as organic amines[17], strong organic acids/amine salts[18], metals and metallic salts[19, 20], alicyclic imide moiety-containing compounds, amide, imide and imidazole[21–25], to facilitate the curing reaction. However, these curing agents volatilizing during the curing reaction will impede the curing reaction and affect the properties of the PN resins especially at elevated temperatures[26]. In our laboratory, the concept of self-promoted curing has been proposed, and amino- or hydroxy-containing phthalonitrile derivatives have been synthesized, solving this above problem to a certain extent[6, 27]. Though a lot of efforts were carried out to face above challenges, however, the application of PN in PCB was rarely reported for relatively high dielectric constant and poor moisture resistance of PN resin[21]. Recently, Laskoski *et al.* and Kaliavaradhan *et al.* synthesized PN containing sulfonyl linkages and bismaleimide (BMI) with a low dielectric constant by molecular design respectively[28, 29].

The polymer blending based on thermoplastic/thermosetting is an important method to broaden the application. In this work, using low polarity rPPO possessing excellent electrical properties to modify the high polarity phthalonitrile resin was carried out in order to obtain cured resins with good thermal properties and improved electrical properties. In order to improve the miscibility, hydroxy-containing low molecular weight PPO, also acting as a curing agent in the blending system, was synthesized. Self-promoted hydroxy-containing phthalonitrile (HPPH) was prepared by an *in situ* method developed in our laboratory previously[30]. The curing behaviors of rPPO-modified phthalonitrile blends were investigated by rheological analysis and infrared (IR) spectroscopy. Moreover, the thermal and dielectric properties of cured rPPO/HPPH were also studied and are reported in this article.

* Corresponding authors: E-mail zk_ican@sina.com (K.Z.)
E-mail yanggang65420@163.com (G.Y.)
Received July 6, 2017; Accepted August 26, 2017; Published online November 16, 2017

EXPERIMENTAL

Materials

PPO (number-average molecular weight $M_n = 3 \times 10^4$ g/mol, M_w/M_n = 1.5) was supplied by Blue Star Chemical New Material of China. Bisphenol A (BPA) and benzoyl peroxide (BPO) were acquired from Chengdu Kelong Chemical Reagent Co. Ltd, Chengdu, China. 4-Nitrophthalonitrile (99%) was purchased from Hong Kong's Ming Tai Prosperity Chemical Co., Ltd. Potassium carbonate (99.0%) was obtained from Chengdu Kelong Chemical Reagent Co., Ltd. All solvents were used without further purification.

Redistribution of PPO with BPA[3]

PPO (40 g) was dissolved in 100 mL of toluene in a four-necked bottle with stirring at 90 °C in nitrogen. Subsequently, 4 g of BPA was added into the solution, and then the solution of 4 g of BPO in 40 mL toluene was added dropwise for 15 min. Following the above procedure, the reaction was kept for another 3 h at 90 °C, then the mixture was cooled to room temperature and was added to methanol to precipitate the product. The pale yellow precipitate was collected by filtration, washed with aq. Na_2CO_3 solution to remove excess BPO, and washed with water and methanol until the filtrate was neutral. Finally, the product was dried at 110 °C in a vacuum oven. The product was obtained in a yield of 70.72%. The M_n value of the redistributed PPO (rPPO) was 1958 g/mol and M_w/M_n = 1.4, as measured with GPC. The T_g of neat rPPO was 119 °C which was measured with DSC. ^{1}H-NMR (300 MHz, $CDCl_3$, δ, ppm): 8.2 (d, 1H; BPA —OH), 7.0–6.8 (m, 4H; BPA Ar—H), 6.45 (s; neat PPO Ar—H), 2.11 (s; neat PPO —CH_3), 1.7 (s, 6H; BPA —CH_3).

Synthesis of Self-promoted Hydroxy-containing Phthalonitrile Systems (HPPH)

To a 500 mL three-necked flask were added 41.52 g of 4-nitrophthalonitrile, 45.6 g of BPA and 400 mL of dimethyl sulfoxide (DMSO). During the course of the reaction, 83 g of pulverized potassium carbonate was added in three portions. The mixture was stirred at 40 °C under nitrogen for 10 h and then poured into 3000 mL of water. The resulting precipitate was collected by filtration, washed with water until the filtrate was neutral, dried at 80 °C under reduced pressure for 16 h. The hydroxy-containing phthalonitrile systems (HPPH) were obtained in a yield of 92%. The m. p. of HPPH were 123 and 166 °C corresponding to HPNM and BAPh respectively. The HPPH was prepared by mixing HPNM and BAPh, as shown in Scheme 1.

Preparation of Polymers

All rPPO/HPPH blends were prepared by mechanical blending. 10-rPPO represents the rPPO/HPPH containing 10 wt% rPPO based on HPPH. The rPPO/HPPH blends were melted in a 100 mL reaction kettle equipped with a stirrer and were degassed under vacuum condition (–0.08 MPa) at 180 °C. The prepolymer was poured into a mold and then cured in a nitrogen-circulation oven with a procedure of curing at 200 °C for 5 h, 230 °C for 5 h, 260 °C for 5 h and 300 °C for 5 h. The cured polymers were machined into rectangular specimens.

Characterizations

^{1}H-NMR spectra were required with a Bruker AV Ⅱ 300 nuclear magnetic resonance (NMR) spectrometer at a proton frequency of 300 MHz. The molecular weights of the rPPO diagrams were obtained using an HLC-8320 GPC Instrument (TOSOH Co., Japan) at 40 °C with two TSK gel columns (Super HM-H S0001/Super HM-H S0002) with tetrahydrofuran as an eluent solvent system. The flow rate was 0.6 mL/min, M_n and M_w values of the samples were calculated on the basis of polystyrene standards. A differential scanning calorimetric (DSC) study was performed on a TA Instruments Q200 DSC at a heating rate of 10 K/min with a nitrogen flow rate of 50 mL/min. The rheological behaviors of the blends were investigated using a TA Instruments Rheometer AR-2000 with a frequency of 1 Hz and a heating rate of 3 K/min. Thermogravimetric analysis (TGA) was performed using a TA Q500 thermogravimetric analyzer at a heating rate of 10 K/min under air and nitrogen atmosphere respectively with a flow rate of 60 mL/min. Dynamic mechanical analysis (DMA) was performed using a TA Instruments Q800 dynamic mechanical analyzer in nitrogen atmosphere from 40 °C to 500 °C with a heating rate of 5 K/min and at a frequency of 1 Hz and a strain of (2.5×10^{-2})%. Fourier transform infrared (FTIR) spectra were obtained from a Nicolet-460 FT-IR spectrometer in KBr pellets. Dielectric measurements were carried out at different frequencies ranging from 10^7 Hz to 10^0 Hz at room temperature using Novocontrol Concept 50 Broadband Dielectric Spectrometer. The morphology of the cured samples was investigated using a Nova·NanoSEM·450 (FEI Instrument, USA) field-emission scanning electron microscope (SEM). The specimens were coated with Au prior to observation.

RESULTS AND DISCUSSION

Preparation

The structure of the HPPH was determined by ^{1}H-NMR spectroscopy, and is shown in Fig. 1. The 60% content of HPNM was calculated using the ^{1}H-NMR integral area of HPPH.

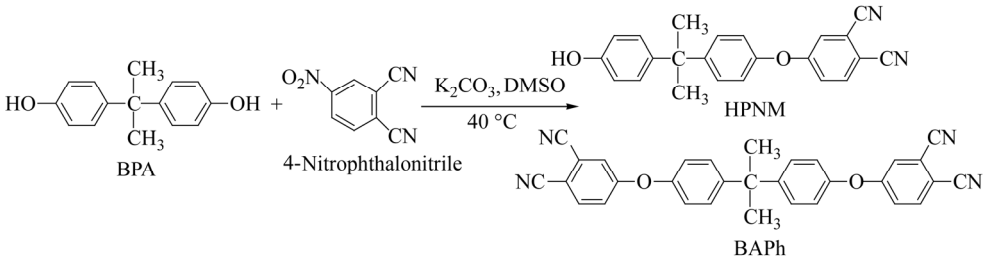

Scheme 1 General synthetic route to HPPH

https://doi.org/10.1007/s10118-018-2026-x

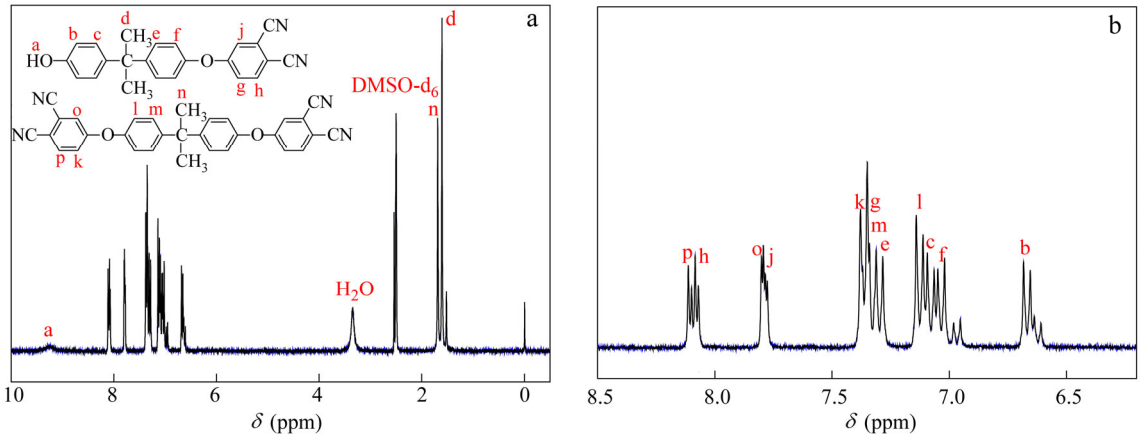

Fig. 1 ^{1}H-NMR spectra of HPPH: (a) from 0 ppm to 10 ppm, (b) local magnification from 6 ppm to 8.5 ppm

$$W_{\mathrm{HPNM}}(\mathrm{mol\%}) = \frac{S_\mathrm{d}}{S_\mathrm{d} + S_\mathrm{n}} \quad (1)$$

The content of HPNM was calculated according to formula (1) (S_d and S_n represent the integral areas d and n in the ^{1}H-NMR spectrum, respectively).

Curing Behavior

The variation in the complex viscosity of the HPPH and rPPO/HPPH blends was measured as a function of temperature from 140 °C to 300 °C. The results, presented in Fig. 2, showed that all the processing windows of the blends were up to 67 °C, which meant that the rPPO/HPPH displayed good processability. Apparently, the curing rate of rPPO/HPPH was slower with the increasing content of rPPO. This may be due to the steric hindrance of the long-chain rPPO, which may reduce the mobility and the reactivity of the —OH on rPPO and HPNM. The increased complex viscosity of the melting rPPO/HPPH caused by rPPO may slow down the rate of the collision between —OH and —CN, resulting in the slower polymerization and formation of crosslinked cured product during the thermal polymerization.

In order to study the curing behavior further, isothermal rheology was carried out at 200, 215 and 230 °C, as shown in Fig. 3. The melt viscosity of the HPPH and rPPO/HPPH blends increased from 0.18 Pa·s to 0.8 Pa·s with the increasing

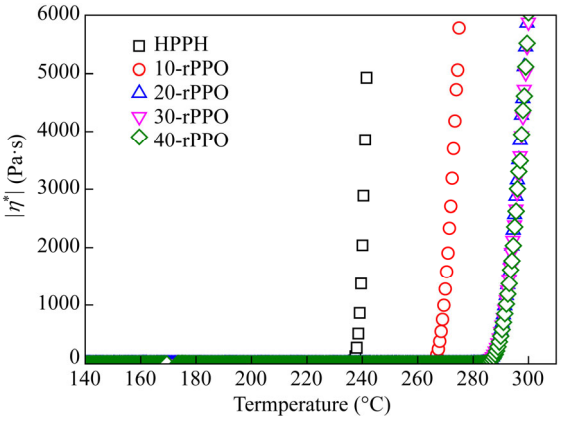

Fig. 2 Complex viscosity ($|\eta^*|$) as a function of temperature for the HPPH and various rPPO/HPPH systems

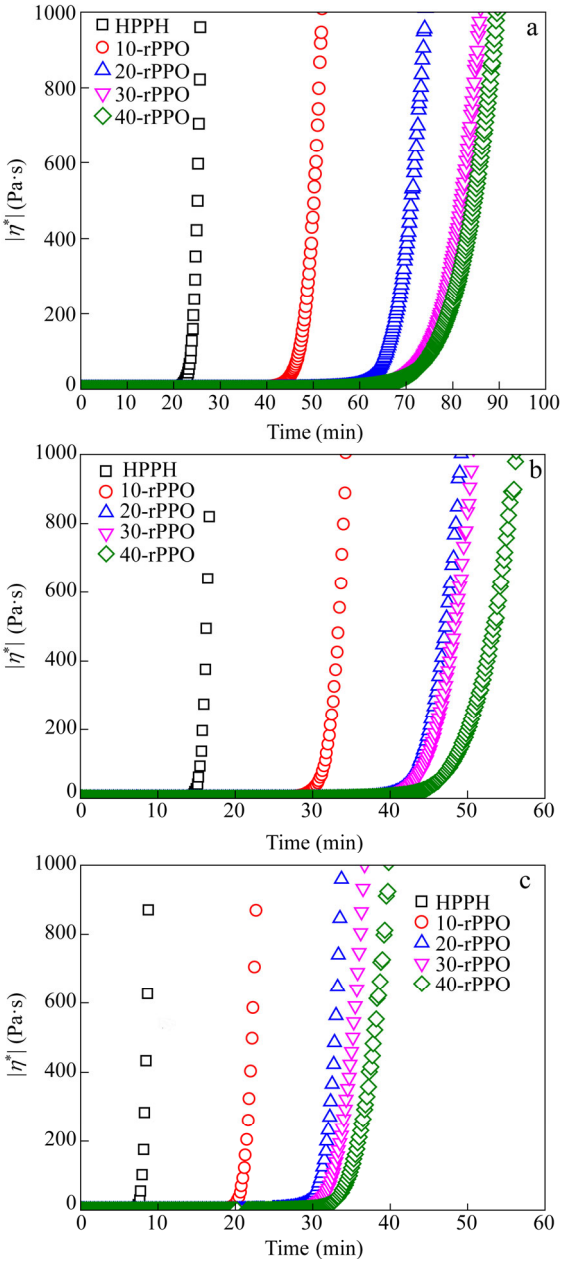

Fig. 3 Melt viscosity versus time curve for HPPH and various rPPO/HPPH systems at (a) 200 °C, (b) 215 °C and (c) 230 °C

https://doi.org/10.1007/s10118-018-2026-x

content of rPPO. The curing rate of blends was faster with the increasing temperature. The elevated temperature may improve the reactivity of —CN and —OH, and enhance the mobility of melting HPPH and rPPO/HPPH blends which may accelerate the rate of the collision and polymerization between —OH and —CN. The higher the content of rPPO, the slower the curing rate was. This may be attributed to the slowing rate of the collision and low reactivity of —OH and —CN. From Fig. 3, the temperature and the content of rPPO had a great impact on the curing rate of all blends.

We further investigated the curing behavior through the analysis of the FTIR spectra of the HPPH and rPPO/HPPH resins, as shown in Fig. 4. From Fig. 4(A), it is obvious that the characteristic absorption band at 2229 cm^{-1} attributed to the —CN was evidently weakened, indicating that the polymerization occurred. Meanwhile new absorption peaks at around 1520 and 1360 cm^{-1} related to triazine were observed. Moreover, typical isoindoline peaks at 1720 and 1090 cm^{-1} were also observed. With the increase of curing temperature, the absorption band of the typical isoindoline and triazine peak enhanced, which indicated that the degree of polymerization was enhanced. All blends cured at 300 °C also had the above typical peaks, indicating that all the system of cured HPPH and rPPO/HPPH possessed isoindoline and triazine, as shown in Fig. 4(B). For the cured HPPH and rPPO/HPPH blends, there was still a weak absorption peak at 2229 cm^{-1}, as shown in Fig. 4. The residual —CN may be attributed to the steric hindrance of the unreacted nitrile groups at the *ortho*-position of triazine ring[18]. Scheme 2 shows the probable curing mechanism of HPPH and rPPO/HPPH system[24].

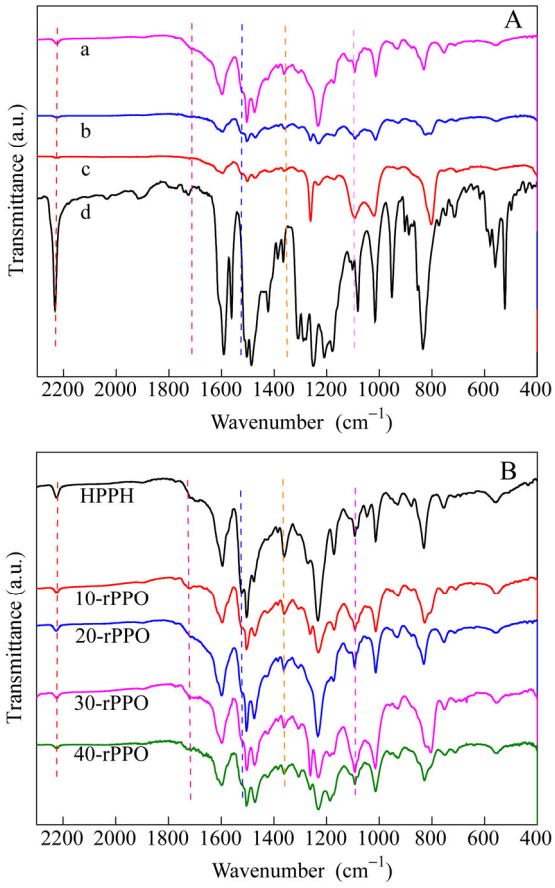

Fig. 4 (A) FTIR spectra of 20-rPPO cured at different temperatures: (a) 200 °C for 5 h, 230 °C for 5 h, 260 °C for 5 h, 300 °C for 5 h; (b) 200 °C for 5 h, 230 °C for 5 h, 260 °C for 5 h; (c) 200 °C for 5 h; (d) uncured 20-rPPO blend; (B) FTIR spectra of HPPH and various rPPO/HPPH cured at 300 °C for 5 h

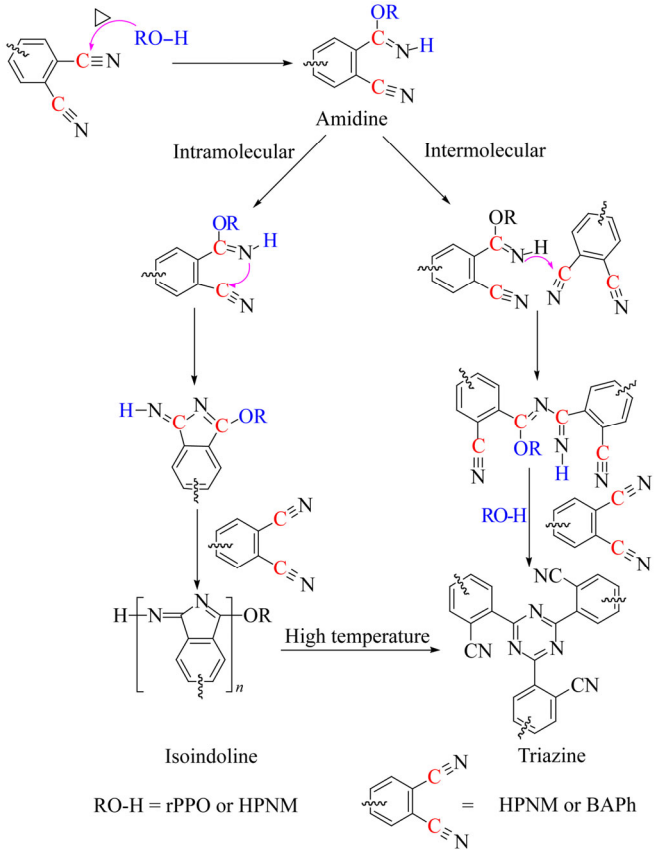

Scheme 2 Probable curing mechanism of HPPH and rPPO/HPPH systems

Morphological Studies

To clearly observe the phase morphology, the fractured surfaces of cured HPPH and rPPO/HPPH were etched with toluene at 120 °C for 18 h in order to remove rPPO phase. The morphologies of cured HPPH and various rPPO/HPPH were observed by SEM and the images are shown in Fig. 5. The morphology of a HPPH polymer is shown in Figs. 5(a) and 5(b). No voids can be observed in the HPPH polymer, proving the void-free structure of the cured HPPH resin. For 10-rPPO, as shown in Figs. 5(c) and 5(d), the fractured surfaces before and after etching showed no clear difference and no voids were left on the etched surfaces. This may imply the occurrence of reaction between the rPPO and HPPH. After etched with toluene, there appeared slight voids on the fractured surface of 20-rPPO, as shown in Figs. 5(e) and 5(f), indicating that the rPPO phase was dispersed in HPPH matrix. The higher content of rPPO may result in a micro-phase separation. For 30-rPPO, as shown in Figs. 5(g) and 5(h), the rPPO was relatively and evenly dispersed in the HPPH matrix and the etched scope was relatively large due to the higher

https://doi.org/10.1007/s10118-018-2026-x

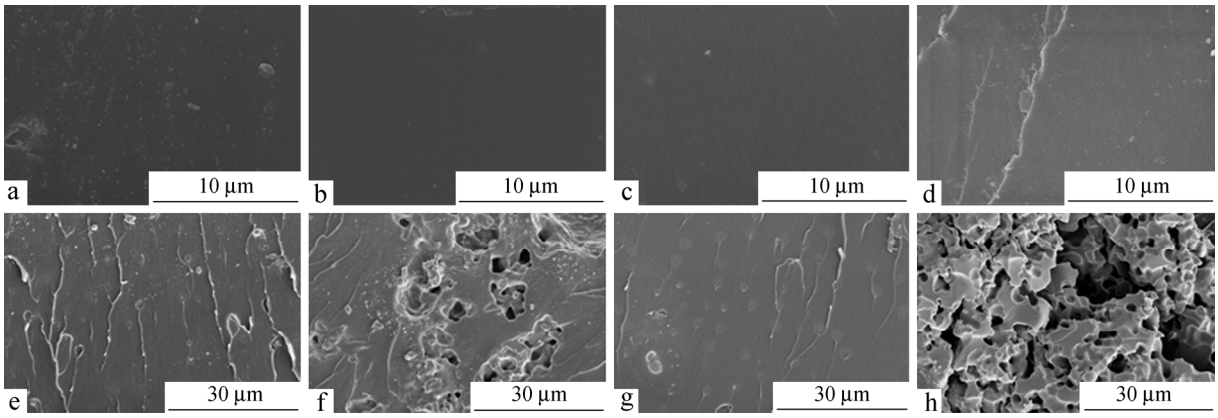

Fig. 5 SEM photographs of the HPPH and various rPPO/HPPH resins cured at 300 °C: (a) HPPH, (b) HPPH (etched), (c) 10-rPPO, (d) 10-rPPO (etched), (e) 20-rPPO, (f) 20-rPPO (etched), (g) 30-rPPO, (h) 30-rPPO (etched)

content of rPPO and the lower cross-link density. From the etched 20-rPPO and 30-rPPO, the separated rPPO phases were not completely chemically bonded to HPPH phase, according to the SEM and DMA.

Thermal Stability

The thermal and thermo-oxidative properties of the cured HPPH and rPPO/HPPH were measured by TGA, and the results are given in Table 1. Whether under a nitrogen atmosphere or under an air atmosphere, the 5 wt% and 10 wt% weight loss temperature presented a decreasing trend with the increasing content of rPPO, expected for 20-rPPO. These data indicated the dependence of the thermal and thermo-oxidative stability on the rPPO content in the blends. For 20-rPPO blend, the $T_{d,5\%}$ under nitrogen and air were higher than those of the other blends. The reason may be that the mobility and the reactivity of the —OH end group were high, and the concentration of —CN was relatively high too when the content of rPPO was 20 wt% based on HPPH. Under the above curing conditions, the rPPO may produce radicals from the broken chain and the end of —OH to facilitate the polymerization of —CN, resulting in a relatively high cross-linking density. The above speculation was based on the following three points: (1) radical may facilitate the polymerization of —CN[21]; (2) the reaction mechanism of the synthesis and redistribution of PPO were carried out by phenoxy radicals and the free radicals were firstly produced from the end —OH under mild conditions[31–35]; (3) PPO could produce poly(2,6-dimethylphenoxy) radicals (PDMP) and a benzylic-type radical as a consequence of thermal energy absorption[36–40]. For 10-rPPO, the content of rPPO was low, so the resulting free radicals to promote the polymerization of —CN were not sufficient to compensate for the reduced thermal performance caused by the addition of rPPO. The concentrations of —CN of 30-rPPO and 40-rPPO were relatively low; besides, the increasing viscosity lowered the rate of the collision and decreased the reactivity of —OH and —CN. Moreover, the addition of rPPO may hinder the heat conduction. This may result in a relatively low cross-linking density, accompanied by the plasticization effect of rPPO. All blends cured at 300 °C exhibited char yields of above 61% when heated under inert conditions at 800 °C, which may endow the resin system with good flame retardant properties. Among them, the 20-rPPO blend also had superior thermal properties to other blends. These results should be attributed to a balance between the crosslinking and plasticization effect of rPPO. The $T_{d,5\%}$ and $T_{d,10\%}$ of all blends in air were higher than those in N_2 from Table 1. The possible reasons are as follows. After the rPPO/HPPH and HPPH blends cured at 300 °C for 5 h, the polymer still had residual —CN groups. Under air conditions, the oxygen free radicals, produced at a higher temperature, may facilitate the polymerization of the residual —CN to a certain extent[21]. On the other hand, degradation temperature and activation energy of PPO were much higher in air than those in nitrogen[37]. From Table 1, the thermal and thermo-oxidative properties of cured HPPH and rPPO/HPPH resins were relatively good.

Dynamic Mechanical Properties

The dynamic mechanical properties of the cured HPPH and rPPO/HPPH polymers were measured to ascertain the modulus and the loss factor (T_g). Plots of the storage modulus (G') and damping factor ($\tan\delta$) are given in Figs. 6(a) and 6(b), respectively. The temperatures of α-mechanical relaxations, $T_{\alpha 1}$ and $T_{\alpha 2}$, related to the glass transition of rPPO and the HPPH networks, are summarized in Table 2. All

Table 1 The TGA data of the HPPH and various rPPO/HPPH resins cured at 300 °C in N_2 and in air at a heating rate of 10 K/min

Resin	TGA in N_2			TGA in air		
	$T_{d,5\%}$ (°C)	$T_{d,10\%}$ (°C)	Char yield at 800 °C (%)	$T_{d,5\%}$ (°C)	$T_{d,10\%}$ (°C)	Char yield at 800 °C (%)
HPPH	391.3	426.4	65.07	402.9	438.2	9.62
10-rPPO	384.0	418.2	61.52	402.4	435.9	1.11
20-rPPO	412.9	446.4	67.75	420.1	459.9	0.85
30-rPPO	379.5	413.0	62.05	399.6	435.3	0.90
40-rPPO	373.4	404.0	61.50	392.1	422.7	0.80

https://doi.org/10.1007/s10118-018-2026-x

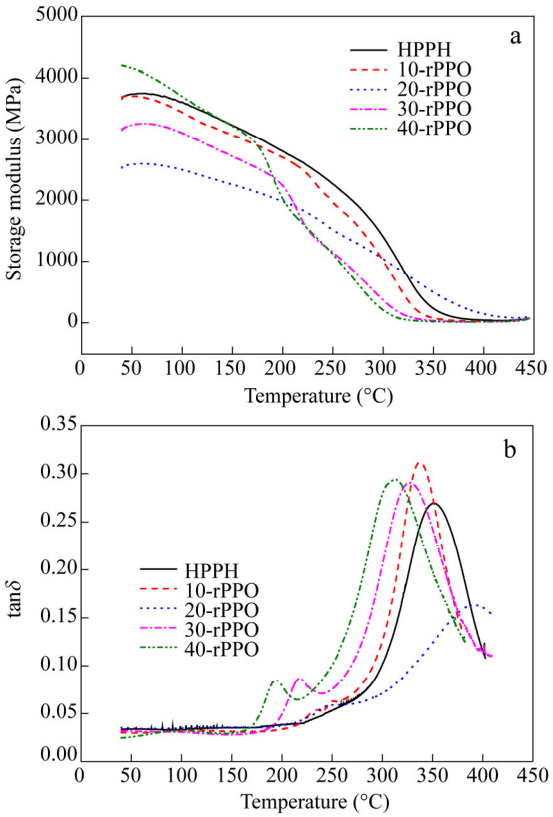

Fig. 6 Dynamic mechanical properties of HPPH and various rPPO/HPPH resins cured at 300 °C: (a) storage modulus versus temperature, (b) tanδ versus temperature

Table 2 The DMA data of HPPH and various rPPO/HPPH resins cured at 300 °C

	HPPH	10-rPPO	20-rPPO	30-rPPO	40-rPPO
$T_{\alpha 1}$ (°C)	–	232, 249	243	216	194
$T_{\alpha 2}$ (°C)	351	338	392	326	314

blends cured at 300°C showed high storage modulus. The high modulus may be credited to the aromatic and crosslinked microstructure. The minimum and maximum modulus were over 2500 and 4500 MPa, respectively, indicating that the mechanical properties of cured HPPH and rPPO/HPPH were good. The DMA curve of cured rPPO/HPPH system exhibited two tanδ peaks. One peak located at above 200 °C was attributed to the glass transition of rPPO segments. This indicated that the rPPO reacted with the —CN group to extend the network chain, contrasting with the glass transition of the neat rPPO observed by DSC. The high T_g may also signify the good thermal and thermo-oxidative properties of cured HPPH and rPPO/HPPH observed by TGA. The other peak located at above 310 °C was attributed to the glass transition of the network of cured HPPH.

From Table 2, the effect of rPPO contents on glass transition is consistent with the $T_{d,5\%}$ observed by TGA under N_2 and air atmosphere. For cured 20-rPPO, the $T_{\alpha 1}$ and $T_{\alpha 2}$ were up to 243 and 392 °C, respectively, which was superior to the other blends, and such difference may be attributed to a balance between the crosslinking and plasticization effect of rPPO. For cured HPPH, 10-rPPO, 30-rPPO and 40-rPPO, the $T_{\alpha 1}$ and $T_{\alpha 2}$ decreased along with the increase of rPPO, which may be due to a dominant plasticization effect of rPPO. The overall network formation involved in rPPO/HPPH curing is depicted in Scheme 3.

Dielectric Constant and Dissipation Factor

The dielectric constant and dielectric factor as a function of frequency for cured samples at room temperature are illustrated in Fig. 7. The dielectric constants measured at 10^7 Hz were 4.51, 4.16, 3.91 and 3.81 corresponding to the cured HPPH, 10-rPPO, 20-rPPO and 30-rPPO, respectively. The difference may be attributed to the low polarity and hydrophobic structure of the rPPO chain, the part rPPO chemically bonded to HPPH phase and low water absorption

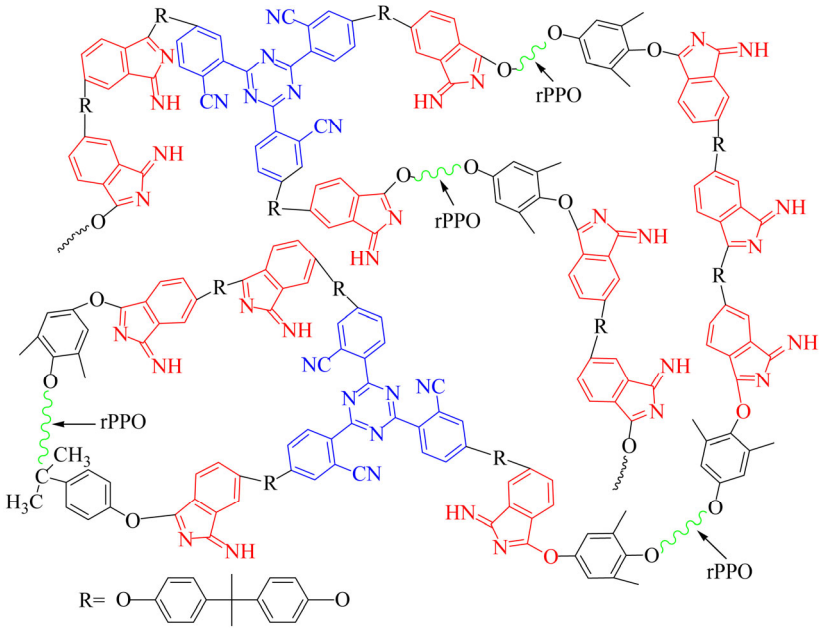

Scheme 3 Likely cured network structure of rPPO/HPPH blends

https://doi.org/10.1007/s10118-018-2026-x

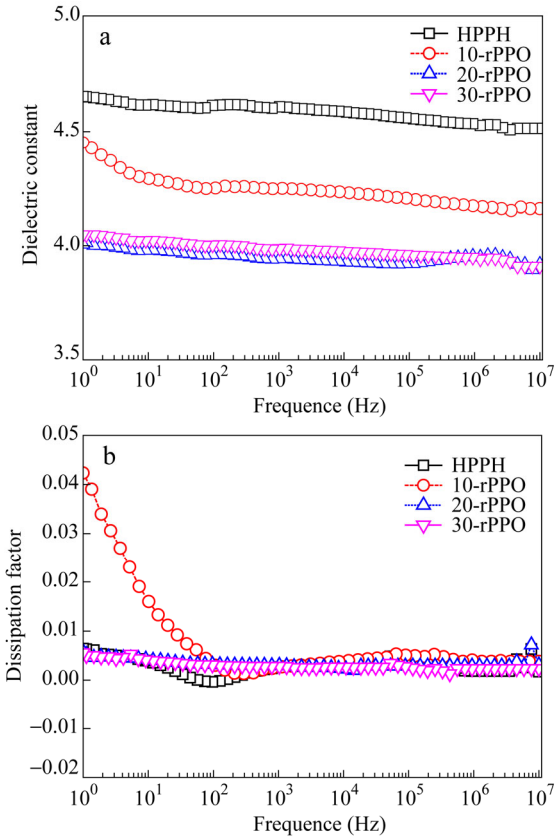

Fig. 7 (a) The dielectric constant and (b) dissipation factor of the HPPH and various rPPO/HPPH resins cured at 300 °C

of the cured rPPO/HPPH. From Fig. 7(a), the addition of rPPO greatly reduced the dielectric constants of HPPH. The measured dissipation factor values at 10^7 Hz were 0.00172, 0.00382, 0.00313 and 0.00236 corresponding to the cured HPPH, 10-rPPO, 20-rPPO and 30-rPPO, respectively, as shown in Fig. 7(b). The dissipation factor of cured HPPH was lower than that of the cured rPPO/HPPH, which may be caused by the interface polarization effect of phase separation. The dissipation factor of cured rPPO/HPPH decreased with the increasing content of rPPO. The difference may also be attributed to the low polarity and hydrophobic structure of the rPPO chain and low water absorption of the cured rPPO/HPPH.

Moisture Resistance

The water absorption capability was measured by absorption experiments in boiling water over a course of 40 h with the 0.8–1 g samples of cured HPPH and various rPPO/HPPH. Figure 8 shows the water absorption of the cured polymers in boiling water. The cured polymers HPPH, 10-rPPO, 20-rPPO and 30-rPPO showed a maximum boiling water amount of approximately 1.53%, 1.46%, 0.92% and 1.26%, respectively, after 40 h immersion. The absorbed moisture of all cured rPPO/HPPH blends was lower than that of HPPH. The difference may be attributed to the low polarity and hydrophobic structure of the rPPO chain. For cured 20-rPPO, the moisture absorption was lower than that of cured 10-rPPO. The phenomenon may be resulted from the higher cross-link density and the higher content of rPPO. Furthermore, the

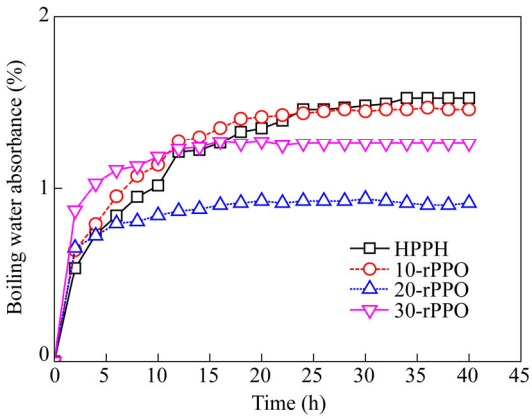

Fig. 8 Boiling water absorption of the HPPH and various rPPO/HPPH resins cured at 300 °C

moisture absorption was also lower than that of cured 30-rPPO. This may be due to the higher degree of phase separation and lower cross-link density of the cured 30-rPPO blend. From Fig. 8, the rPPO greatly reduced the moisture absorption of HPPH system.

CONCLUSIONS

The rPPO was used to modify HPPH without compatibilizer and the resulting polymers showed partly chemical bonded phase separation. The cured rPPO/HPPH showed good thermal and mechanical properties. The increasing content of rPPO greatly improved the moisture resistance and reduced the dielectric property. The prepared rPPO/HPPH polymer network exhibited high modulus and high T_g of 392 °C. And the rPPO/HPPH system also showed a large processing window (over −67 °C).

This study may open up a new research direction of the PN application to PCB through blending.

ACKNOWLEDGMENTS

This work was financially supported by the National Natural Science Foundation of China (Nos. 51203098 and 51173114).

REFERENCES

1 Seike, Y.; Okude, Y.; Iwakura, I.; Chiba, I.; Ikeno. T.; Yamada, T. Synthesis of polyphenylene ether derivatives: estimation of their dielectric constants. Macromol. Chem. Phys. 2003, 204(15), 1876–1881.
2 Liang, G. Z.; Meng, J.; Zhao, L. Synthesis of styrene-maleic anhydride random copolymer and its compatibilization to poly(2,6-dimethyl-1,4-phenylene ether)/brominated epoxy resin. Polym. Int. 2010, 52(6), 966–972.
3 Hwang, H. J.; Hsu, S. W.; Wang, C. S. Synthesis and physical properties of low-molecular-weight redistributed poly(2,6-dimethyl-1,4-phenylene oxide) for epoxy resin. J. Appl. Polym. Sci. 2008, 110(3), 1880–1890.
4 Su, C. T.; Lin, K. Y.; Lee, T. J.; Liang, M. Preparation, characterization and curing properties of epoxy-terminated poly(alkyl-phenylene oxide)s. Eur. Polym. J. 2010, 46(7), 1488–1497.
5 Ishii, Y.; Ryan, A. J. Processing of poly(2,6-dimethyl-1, 4-phenylene ether) with epoxy resin. 1. Reaction-induced phase

separation. Macromolecules 2000, 33(1), 158–166.
6 Zeng, K.; Zhou, K.; Zhou, S. H.; Hong, H. B.; Zhou, H. F.; Wang, Y. P.; Miao, P. K.; Yang, G. Studies on self-promoted cure behaviors of hydroxy-containing phthalonitrile model compounds. Eur. Polym. J. 2009, 45(4), 1328–1335.
7 Laskoski, M.; Dominguez, D. D.; Keller, T. M. Synthesis and properties of a bisphenol A based phthalonitrile resin. J. Polym. Sci., Part A: Polym. Chem. 2005, 43(18), 4136–4143.
8 Dominguez, D. D.; Keller, T. M. Phthalonitrile-epoxy blends: cure behavior and copolymer properties. J. Appl. Polym. Sci. 2010, 110(4), 2504–2515.
9 Sastri, S. B.; Keller, T. M. Phthalonitrile polymers: cure behavior and properties. J. Polym. Sci., Part A: Polym. Chem. 1999, 37(13), 2105–2111.
10 Augustine, D.; Mathew, D.; Nair, C. P. R. Phenol-containing phthalonitrile polymers-synthesis, cure characteristics and laminate properties. Polym. Int. 2013, 62(7), 1068–1076.
11 Lv, J. B.; Ma, J. Z.; Cheng, K.; Chen, C.; Hu, J. H.; Zeng, K.; Yang, G. Insights into phthalonitrile/epoxy blends modification system from non-competitive cure system based on alicyclic anhydride. Chinese J. Polym. Sci. 2017, 35(12), 1561–1571.
12 Zhou, H.; Badashah, A.; Luo, Z. H., Liu, F.; Zhao, T. Preparation and property comparison of ortho, meta, and para autocatalytic phthalonitrile compounds with amino group. Polym. Adv. Technol. 2011, 22(10), 1459–1465
13 Laskoski, M.; Dominguez, D. D. Keller, T. M. Synthesis and properties of aromatic ether phosphine oxide containing oligomeric phthalonitrile resins with improved oxidative stability. Polymer 2007, 48(21), 6234–6240.
14 Sastri, S. B.; Armistead, J. P.; Keller, T. M. Phthalonitrile-carbon fiber composites. Polym. Compos. 1996, 17(6), 816–822
15 Sastri, S. B.; Armistead, J. P.; Keller, T. M. Phthalonitrile-glass fabric composites. Polym. Compos. 1997, 18(1), 48–54.
16 Dominguez, D. D.; Jones, H. N.; Keller, T. M. The effect of curing additive on the mechanical properties of phthalonitrile-carbon fiber composites. Polym. Compos. 2004, 25(5), 554–561.
17 Keller, T. M.; Price, T. R. Amine-cured bisphenol-linked phthalonitrile resins. J. Macromol. Sci. Chem. 1982, 18(6), 931–937.
18 Burchill, P. J. On the formation and properties of a high-temperature resin from a bisphthalonitrile. J. Polym. Sci., Part A: Polym. Chem. 1994, 32(1), 1–8.
19 Keller, T. M.; Griffith, J. R. The synthesis of a new class of polyphthalocyanine resins. J. Am. Chem. Soc. 1980, 132, 25–34.
20 Walton, T. R.; Griffith, J. R.; O'Rear, J. G. Adhesion science and technology. J. Adhes. Sci. Technol. 1975, 9, 665–676.
21 Yuan, P.; Ji, S. C.; Hu, J. H.; Hu, X. P.; Zeng, K.; Yang, G. Systematic study on highly efficient thermal synergistic polymerization effect between alicyclic imide moiety and phthalonitrile: scope, properties and mechanism. Polymer 2016, 102, 266–280.
22 Ji, S. C.; Yuan, P.; Hu, J. H.; Sun, R.; Zeng, K.; Yang, G. A novel curing agent for phthalonitrile monomers: Curing behaviors and properties of the polymer network. Polymer 2016, 84, 365–370.
23 Hu, J. H.; Wu, D. M.; Lu, D. K.; Xiang, S. R.; Zhao, Y. C.; Zeng, K.; Yang, G. Study on thermal behaviors of a novel cruciform amide-containing phthalonitrile monomer. Des. Monomers Polym. 2015, 18(7), 620–626.
24 Hu, J. H.; Liu, Y. C.; Jiao, Y.; Ji, S. C.; Sun, R.; Yuan, P.; Zeng, K.; Pu, X. M.; Yang, G. Self-promoted phthalimide-containing phthalonitrile resins with sluggish curing process and excellent thermal stability. RSC Adv. 2015, 5(21), 16199–16206.
25 Wu, D. M.; Zhao, Y. C.; Zeng, K.; Yang, G. A novel benzimidazole-containing phthalonitrile monomer with unique polymerization behavior. J. Polymr. Sci., Part A: Polym. Chem. 2012, 50(23), 4977–4982.
26 Sastri, S. B.; Keller, T. M. Phthalonitrile cure reaction with aromatic diamines. J. Polym. Sci., Part A: Polym. Chem. 1998, 36(11), 1885–1890.
27 Zeng, K.; Zhou, K.; Tang, W. R.; Tang, Y.; Zhou, H. F.; Liu, T.; Wang, Y. P.; Zhou, H. B.; Yang, G. Synthesis and curing of a novel amino-containing phthalonitrile derivative. Chinese Chem. Lett. 2007, 18(5), 523–526.
28 Laskoski, M.; Keller, T. M.; Ricks-Laskoski, H. L.; Giller, C. B.; Hervey, J. Improved synthesis of oligomeric sulfone-based phthalonitriles. Macromol. Chem. Phys. 2015, 216(17), 1808–1815.
29 Kaliavaradhan, K.; Muthusamy, S. Synthesis and characterization of various phenylene diamine-based bismaleimide-containing phthalonitrile resins. Polym. Bull. 2016, 7(73), 1921–1938.
30 Wang, J. B.; Hu, J. H.; Zeng, K.; Yang, G. Preparation of self-promoted hydroxy-containing phthalonitrile resins by an in situ reaction. RSC Adv. 2015, 5(127), 105038–105046.
31 Bolon, D. A. Free-radical redistribution of phenol dimers. J. Org. Chem. 1967, 32(5), 1584–1590.
32 Aert, H. A. M. V.; Genderen, M. H. P. V.; Steenpaal, G. J. M. L. V.; Nelissen, L.; Meijer, E. W. Modified poly(2,6-dimethyl-1,4-phenylene ether)s prepared by redistribution. Macromolecules 1997, 30(20), 6056–6066.
33 Baesjou, P. J.; Driessen, W. L.; Challa, G.; Reedijk, J. A kinetic and spectroscopic study on the copper catalyzed oxidative coupling polymerization of 2,6-dimethylphenol. X-ray structure of the catalyst precursor tetrakis (*N*-methylimidazole) bis(nitrato) copper(II). J. Mol. Catal. A-Chem. 1996, 110(3), 195–210.
34 Hay, A. S. Polymerization by oxidative coupling: discovery and commercialization of PPO and noryl resins. J. Polym. Sci., Part A: Polym. Chem. 1998, 36(4), 505–517.
35 Viersen, F. J.; Challa, G.; Reedijk, J. Mechanistic studies of the oxidative coupling polymerization of 2,6-dimethylphenol: 4. Mechanism of polymer formation catalysed by a copper(II)-tmed complex. Polymer 1990, 31(7). 1368–1373.
36 Scoponi, M.; Pradella, F.; Kaczmarek, H.; Amadelli, R.; Carassiti, V. A reappraisal of the photo-oxidation mechanism at short and long wavelengths for poly(2,6-dimethyl-1,4-phenylene oxide). Polymer 1996, 37(6), 903–916.
37 Li, X. G. High-resolution thermogravimetry of poly(2, 6-dimethyl-1,4-phenylene oxide). J. App. Polym. Sci. 1999, 71(11), 1887–1892.
38 Blanco, I.; Cicala, G.; Latteri, A.; Mamo, A.; Recca, A. Thermal and thermo-oxidative degradations of poly (2,6-dimethyl-1,4-phenylene oxide) (PPO)/copoly(aryl ether sulfone) P(ESES-*co*-EES) block copolymers: a kinetic study. J. Therm. Anal. Calorim. 2013, 112(1), 375–381.
39 Saron, C.; Sanchez, E.; Isabel Felisberti, M. Thermal and photochemical degradation of PPO/HIPS blends. J. Appl. Polym. Sci. 2007, 104(5), 3269–3276.
40 Saron, C.; Felisberti, M. I. Dynamic mechanical spectroscopy applied to study the thermal and photodegradation of poly(2,6-dimethyl-1,4-phenylene oxide)/high impact polystyrene blends. Mat. Sci. Eng. A 2004, 370(1), 293–301.

https://doi.org/10.1007/s10118-018-2026-x